N.P.Sell@bath.ac.uk

Accuracy Evaluation of a Drill Guidance System for Orthopaedic Surgery

Nathan P. Sell · Ioannis Georgilas · James Bridgwater-Court · Grey Giddins · Jonathan du Bois

Received: date / Accepted: date

Abstract When placing a screw or wire (K-wire) into bone orthopaedic surgeons attempt to make the first drill pass the only drill pass. This is difficult, however, as they are dealing with complex 3-dimensional shapes with limited access due to the soft tissues. In current practice intra-operative fluoroscopy is used to assist the surgeon but this is limited to 2-dimensional images for the majority of Operating Rooms (OR). This results in multiple attempts in order to achieve optimal positioning, making the process time-consuming and potentially damaging to the soft tissue and bone, resulting in excessive removal of material from the bone, as well exposing the OR staff to increased doses of radiation. Although there are existing tracking methods using optical or forced-based techniques these are time-consuming to setup, suffer from occlusions or lowered precision depending on conditions. This paper documents the initial development of a Drill Guidance System (DGS) to help surgeons drill into bones, especially smaller ones, accurately at the first attempt using a localised vision-based approach. The proposed system can be used easily retrofitted to existing drilling equipment and, being localised to the surgical field, is not prone to accidental occlusions during operation. We are presenting original laboratory results which demonstrate that for usable drilling distances for screw/wire placements of 300mm and 400mm, accuracies of 0.45±0.56mm and 0.39±1.2mm respectively can be achieved which is safely below the desired accuracy of 2mm as set by discussions with surgeons.

Keywords Orthopaedic Surgery · Machine Vision · Computer Assisted Surgery · Surgical Guidance

N.P.Sell
Dept. Mechanical Engineering
University of Bath
Bath, UK
BA2 1AY

1 Introduction

One of the most common operations in orthopaedic surgery is the drilling of bones for fracture fixation. The surgeon is using a pneumatic or electric drill to place Kirschner wires (K-wires) and screws to secure bone fragments. These can secure other metal components (usually plates) to ensure stability or used on their own for smaller and more delicate fractures. For example, in the case of the scaphoid [6] the surgeon has to place percutaneously a guidance K-wire along the longitudinal axis of the scaphoid and across the fracture site and then use this to guide a cannulated screw to secure the fracture. In this case drilling accuracy is very important to ensure that minimum damage to soft-tissue as well as minimum removal of bone tissue is ensured. The exact placement of the screw can affect the quality of the surgical outcome and this in turn impacts patient health and costs of further treatment.

The current practice is for surgeons to use 2-dimensional imaging with pre-operative radiographs (X-rays) for planning and intra-operative fluoroscopy (C-arm) for guidance. This can work adequately, but not infallibly, for large, simple shaped bones but not with smaller, complex shaped bones such as the scaphoid, distal humerus and talus. In such cases, surgeons are required to re-drill multiple times into a bone before they are satisfied with the placement. Three to five attempts per hole is common even for experienced surgeons, particularly on smaller bones. This increases the duration of surgery which in turn increases the risks for the patient and increases costs. Inaccurate drilling can also damage delicate tissue around the bone, leading to complications for the patient [7], especially in fractures involving a bone with an articulation surface [3]. Even with patience and experience, imperfect screw positioning may be (or must be) accepted as the previous drill holes guide the drill into the previous drill tracks making repositioning difficult. In addition, patients and Operating Room (OR) staff are exposed to increased radiation, as each drilling attempt requires at least two fluoroscopic images, usually an anteroposterior (AP) and a lateral view, to ensure that the axis of the drilling tool is aligned with the desired drilling axis, and even a higher number in complex cases [11].

There is a number of solutions that are trying to assist the surgeon in performing drilling operations but mainly aim for complex and sensitive areas [5]. These methods in their original version were using force-sensing techniques to detect penetration of the cortical part of the bone [1, 2] to update the surgeon on the status of the operation. The later versions moved more closely to using full-robotic solutions to perform the critical elements of the procedure under the supervision of the surgeon [10, 15]. Finally, there is a number of solutions that have reached the market and are aiming for performing spine operations under image-guided conditions like the Renaissance (Mazor Robotics Ltd. Caesarea, Israel) and iSYS 1 (iSYS Medizintechnik GmbH, Kitzbuehel, Austria) systems. Another category of computer and robotic assisted orthopaedic operation is arthoplasty. There are image-free hand-held solutions using visual markers (fiducials) [9] or semi-autonomous solutions like the Mako Robotic-Arm Assisted Surgery (Stryker, Kalamazoo, USA) described in [12].

These systems involve use of multiple pre-operative scanning modalities (CT-scanning, X-rays), expensive and bulky computer equipment and setting up (optical trackers) making them not practical for treatment of fractures, especially for non-elective cases. There is a need for a system that can improve accuracy over current freehand methods with little prior set-up, while offering long-term benefits through reduced operative time and fewer complications. It has been proposed previously that such a system could be realised using fiducial markers and existing computer vision algorithms [8]. This paper documents the initial development of the proposed Drilling Guidance System (DGS) and the experimental evaluation of the system's accuracy.

2 System Overview

2.1 DGS system details

The DGS system is made up of a tracking unit which is attached to the orthopaedic drill and a probe with fiducial markers attached. The tracking unit attached to the drill itself is comprised of five main elements:

1. Sterilisable housing
2. Processing unit
3. Camera and optics
4. Touch-screen
5. Battery

All the other components are located within the sterilisable housing, a concept design of which can be seen in Figure 1.

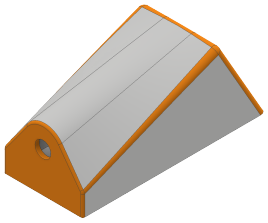

Fig. 1: Drill Guidance System sterilisable housing

The probe, which is used to indicate the desired exit point, could take a number of forms but for ease of use and manufacture it is currently envisioned as a standard surgical probe with a plastic cube affixed to the top with markers on each face. A model can be seen in Figure 2.

Aruco markers [13] were selected for this project due to the extensive literature, availability in both Python and C++ and reported low detection times.

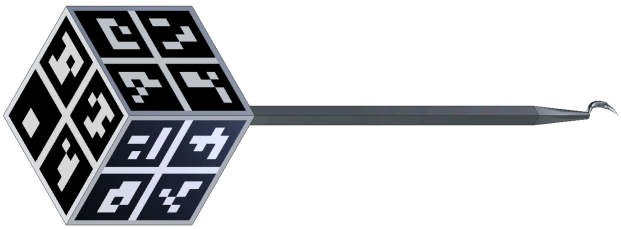

Fig. 2: Drill Guidance System probe

Details of how markers are detected can be found in the Aruco documentation [14] and will not be discussed. However, pose estimation will be reviewed due to its direct effect on the DGS' accuracy

In order to estimate 3D information from 2D images (pose estimation) it is necessary to understand the characteristics of the camera and lens combination used. This is achieved by mapping known 3D world points to corresponding 2D points, this is often achieved using a chequerboard of known size. The relative locations of the squares corners are known in the real world and their 2D location can be found in the 2D image due to the marked change from black to white at the corner locations. The accuracy with which these corners are found naturally impacts the accuracy of the calibration. Therefore, subpixel refinement algorithms are used to estimate the most likely location of a corner within a pixel. There are a number of methods to achieve this but the chosen method is implemented within OpenCV. The accuracy with which the calibrated model of the camera and lens arrangement represents the physical system is quantified by the mean re-projection error. This is the mean difference between the corner locations found by the subpixel corner algorithm and the corner locations that would be expected based on the calibrated model.

Once this calibration has been found it, plus the corner locations of each marker (found using the same subpixel corner method as used in calibration) and the known dimensions of the marker are used by the Aruco library to calculate the Rodriguez rotation [4] and translations which would map the camera frame of reference onto the marker's frame of reference. This method is naturally very sensitive in inaccuracy in the detection of corner positions. This problem can be exacerbated by the construction of the markers because the subpixel algorithm can resolve to an incorrect corner if the search area of the algorithm is large enough. This can be seen in Figure 3.

Within the Aruco library it is possible to improve the accuracy of pose estimation by using marker boards instead of single markers. A marker board is a number of identically sized markers with known spacing between them. Figure 4 shows a marker board made up of 2 x 2 14mm Aruco markers with 2mm spacing.

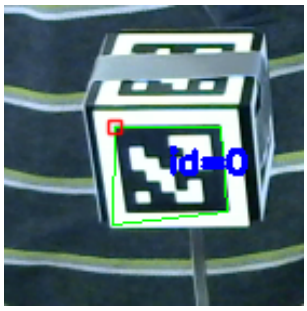

Fig. 3: Incorrect corner from subpixel refinement

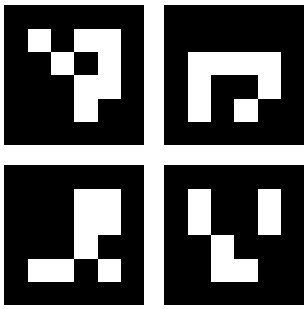

Fig. 4: Aruco marker board

As the board is made of multiple markers and known sizing of white space its pose can be more accurately estimated as it is less sensitive to errors in individual corners or part obscuring on markers. However, using the same size markers the board is significantly larger than one individual marker which leads to a trade-off between size and accuracy as larger individual markers are also generally more accurate for pose estimation.

Assuming the pose of a marker can be accurately estimated it is still necessary to use this information to guide the tip of the drill to the point of the probe instead of the camera to the center of the marker. Therefore, additional calibration will be necessary. The relationship between probe tip and marker (or board) centre could be determined in the manufacturing of the probes but as the unit is intended to be retrofitted to existing drills the relationship between camera and drill tip must be calculated after installing the device onto a drill.

2.2 Clinical Workflow

The use of the DGS in the clinical context will consist of two distinctive phases, the setup, and the operation phase. In the setup phase, the tracking unit of the DGS is placed on the available drill following OR procedures to ensure

sterilisation and the sterilised DGS probe is made available to the surgeon along with the other surgical tools. The positioning of the tracking unit on the drill will be either unique for the drill or a fast, automated calibration process will take place before the start of the operation.

In the tracking phase, the surgeon will place the K-wire or screw on the drill and this will be registered by the DGS tracking unit. Following this, the surgeon will select an exit point on the operated bone and place the tip of the DGS probe on this while placing the wire/screw tip on the entrance point. The final step will be to pivot the drill so they can align the tip with the exit point, using the indication on the tracking unit. The unit will be calculating the desired motion to achieve the alignment (e.g. pivot left/right/up/down) based on the information from the visual system as interpreted by the fiducal markers.

3 Experimental Set-up

In order to verify that the underlying libraries on which the DGS is built are capable of achieving the 2mm target accuracy bench testing was undertaken within the University of Bath. Figure 5 shows the camera set-up:

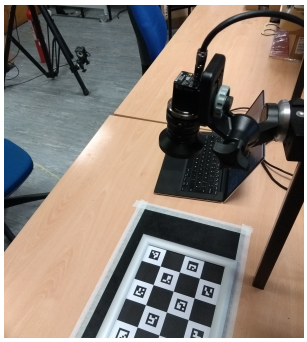

Fig. 5: Experimental camera set-up

The camera used for all results within this paper is the Ximea MQ042CG-CM with a KOWA LM8HC lens attached. The iris of the lens was set at the beginning of the tests and then locked in place while focus was varied as required. No local lighting was used in the gathering the results as it is not intended to be part of the DGS system.

The Matlab tool was used to realise the calibration used through-out this report. Equation 1 shows the camera matrix and distortion coefficients found and Figure 6 shows the mean re-projection errors for each image.

$$
\begin{aligned}
camera\ matrix &= \begin{bmatrix} 1476.5 & 0 & 1017.3 \\ 0 & 1480.3 & 1003.5 \\ 0 & 0 & 1 \end{bmatrix} \\
radial\ distortion &= [-0.1678, 0.1131, -0.0238] \\
tangential\ distortion &= [-8.701, 5.569] \times 10^{-4}
\end{aligned} \tag{1}
$$

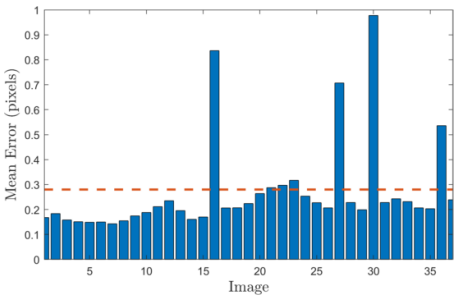

Fig. 6: Camera calibrations re-projection errors

Attempting to accurately record the location of the camera and markers in 3D space in order to test the system accuracy would be both time consuming and challenging. Moreover such a calibration method is impractical in the target application environment, i.e. in an OR. Therefore, an approach similar to that used for calibration was taken using the relative pose of 24 boards of markers which were laser printed onto an A4 sheet instead of the absolute pose of a marker board with respect to the camera. Two assumptions are inherent in using the relative pose. Firstly, that the spacing between the boards is known perfectly and secondly that the paper is perfectly flat in all images captured meaning all boards have the same orientation. There will some error in results due to these assumptions, with the marker size likely to vary slightly from expected (due to printing) and whilst the sheet of paper was clamped along each of its edges it is likely that there was still some variation in the markers' orientation across the sheet Both of these are assumed to be insignificant.

The marker boards used each featured 4 markers of 14mm with 2mm of white space between markers. This enables a probe with marker cube of 35mm to be realised which is the smallest probe expected to be required (and therefore the least accurate). They were printed in a grid of 4 horizontal and 6 vertical with equal spacings of 48mm x 41mm respectively. The translational error of each board was calculated by taking the mean of the absolute error between from the board to all other boards. The rotational errors were found by converting the Rodriguez rotation returned by Aruco into Euler angles and finding the difference between each board's angles and the mean angles of all other boards. The rotational and translational errors were then combined to

give the total error in drill tip position that would be expected due to these errors. The equations used by the algorithm for doing this can be found in Equation 2.

$$\begin{aligned} \Delta x_\theta &= \sqrt{2 \cdot x_{probe}^2 (1 - cos(\Delta\theta_x))} \\ \Delta y_\theta &= \sqrt{2 \cdot y_{probe}^2 (1 - cos(\Delta\theta_y))} \\ \Delta z_\theta &= \sqrt{2 \cdot z_{probe}^2 (1 - cos(\Delta\theta_z))} \\ \sum Error &= \sqrt{\Delta x_\theta^2 + \Delta y_\theta^2 + \Delta z_\theta^2 + \Delta xyz} \end{aligned} \tag{2}$$

where x_{probe} is the distance between the tip of the probe and the centre of rotation in the x-axis. It is assumed within this paper that $x_{probe} = z_{probe}$=150mm and that y_{probe} =0mm as the tip can be directly under the centre of the marker cube.

4 Results

Figure 7 shows an original image of the Aruco boards and its undistorted counterpart.

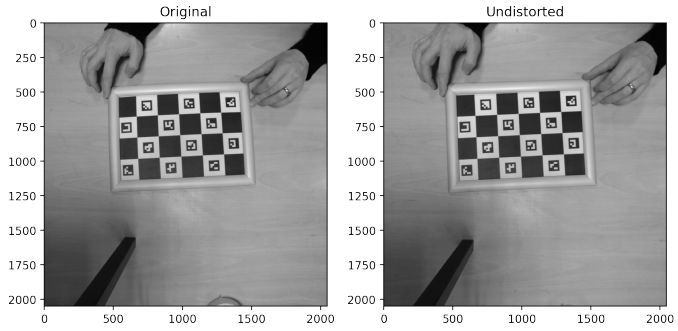

Fig. 7: Effect of camera calibration

A series of 140 test images were captured with the board 300mm from the camera. The relative error of single markers within a board was then compared with the inter-board error, Figure 8.

It is clear that using boards provides an advantage, despite the sample size being reduced as only images where all markers were detected were used, justifying the desire to use boards. Figure 9 shows the total error from a selection of boards across the images taken.

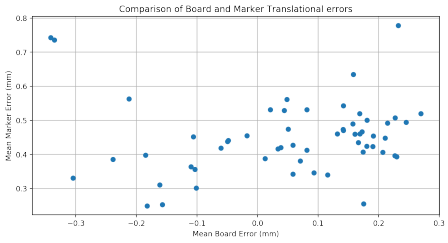

Fig. 8: Comparison of marker and board error

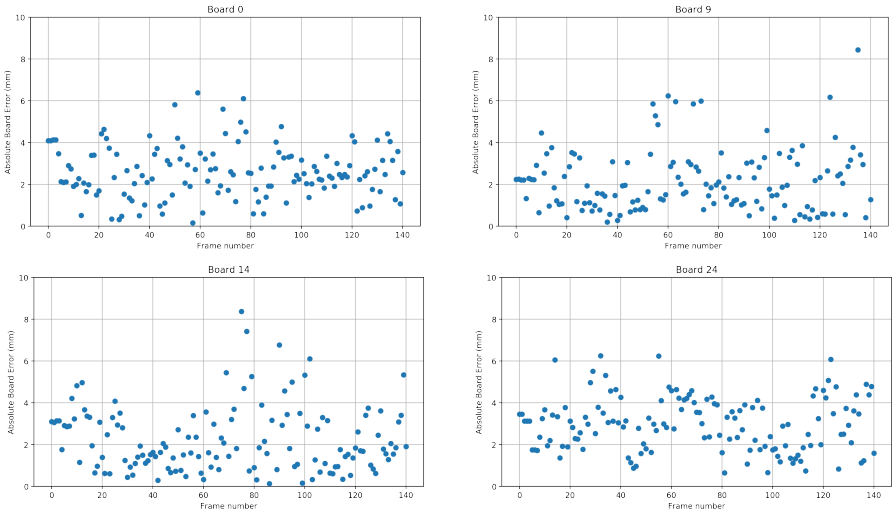

Fig. 9: Total error of boards

It can be seen that the total error is significantly greater than the target error for the DGS. Figure 10 shows the constituent parts of the error for one of the boards.

It can be seen that the greatest contribution comes from error in rotation around Z. This is a result of a limitation with fiducial markers as using only a single image allows for two possible mirrored versions of the Z axis. This limitation is discussed in the Aruco documentation [14] and means that the method of determining the correct orientation from the mean of all other boards in the image is invalid for the Z direction as the errors in each board are not Gaussian but deterministic. In use this is less of a concern as the flip can be easily detected from frame to frame and corrected. If the Z error is replaced by the X error (which should be representative of the error without the issue of Z axis mirroring) then the total error reduces significantly.

As mentioned in Section 2 the final accuracy of pose estimation is highly dependant on the sub-pixel refinement method used to determine the corner positions. Thus far all the results have used the OpenCV sub-pixel refinement

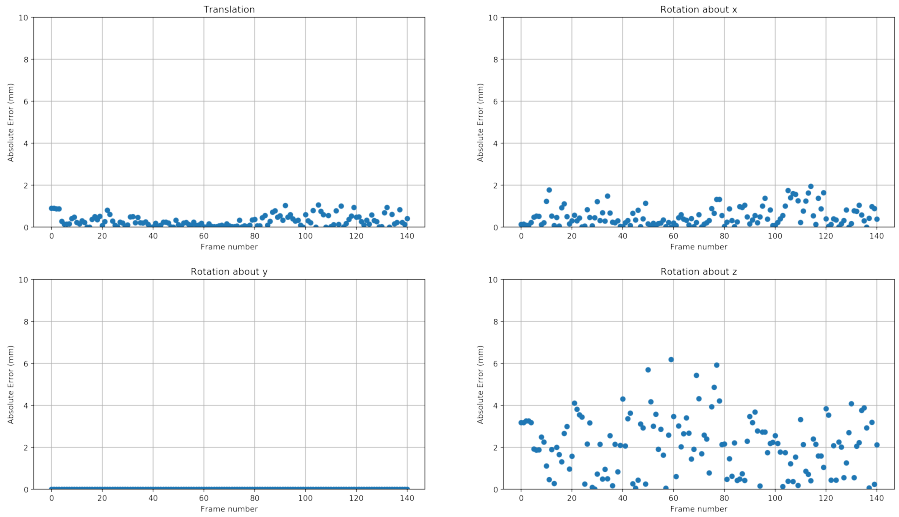

Fig. 10: Constituent errors for a board

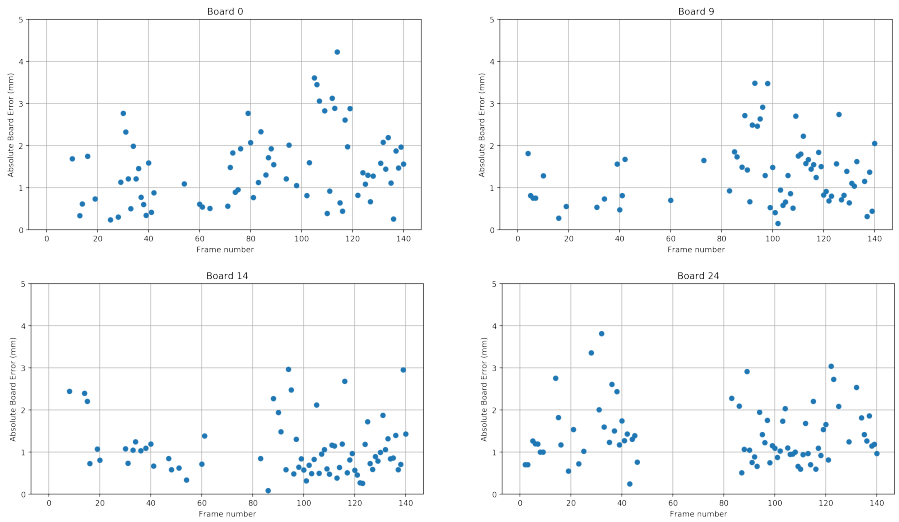

Fig. 11: Total error of boards without Z axis mirroring

algorithm with its default settings which uses 5 rows and columns of pixels surrounding the detected corner to refine its location to a sub-pixel accuracy. Figure 12 shows how the mean accuracy and standard deviation were affected by changes to these settings.

The results show little improvement in accuracy from considering more than 4 rows and columns of pixels and also indicate that ignoring the detected pixel and those immediately surrounding it improve accuracy further.

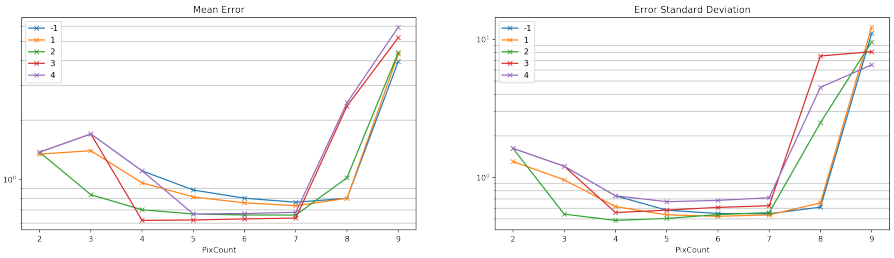

Fig. 12: Effect of sub-pixel settings on DGS accuracy

Using these settings with the 140 images captured provides a mean accuracy of 0.45mm and standard deviation of 0.56mm, Figure 13

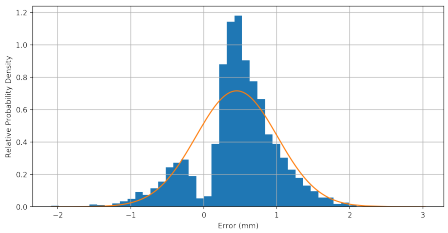

Fig. 13: Error with boards 300mm from camera

When the same test is conducted with 400mm between the camera and board the mean accuracy reduces to 0.39mm but the standard deviation increases to 1.2mm.

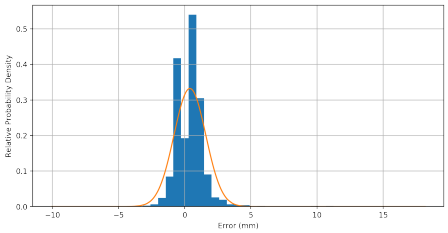

Fig. 14: Error with boards 400mm from camera

Moving to 500mm from the camera, results in a large increase in standard deviation to 59.36mm, whilst the mean error increases slightly to 8.64mm. This is largely due to markers not being detected in each image giving rise to some boards having errors of over 30mm (nearly a whole marker of shift). It these are discounted then there is a marked improvement in the results, with

mean error becoming 1.85mm with a standard deviation of 2.85mm, Figure 16.

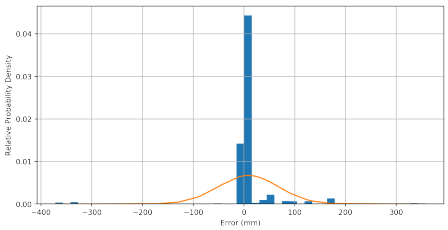

Fig. 15: Error with boards 500mm from camera

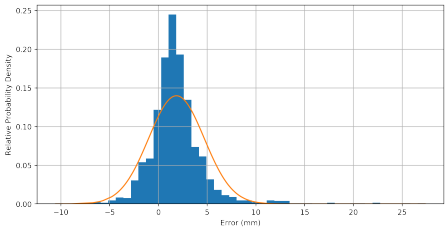

Fig. 16: Error with boards 500mm from camera with all markers detected

5 Discussion

With the current experimental set-up it has been possible to achieve the 2mm accuracy target with the marker board 300mm away from the camera, for a large number of surgical procedures this would likely prove sufficient. For surgery on larger bones this may be a limiting factor but the required accuracy is also generally lower in these cases. If the variation in accuracy with distance is categorised then information can be relayed to the user allowing them to make an informed decision on moving the probe closer to the camera or accepting the reduction in accuracy.

In order to achieve the accuracies stated above it is necessary to detect and mitigate the mirroring of the z-axis. This should be possible as the instant where the z-axis flips should be detectable as an unreasonable jump which would allow the z-axis to then be mirrored before the probe's pose is determined. It was also found that, unsurprisingly, pose estimation was much higher when all markers were detected and that there was a loose trend between marker and board accuracy. This information could be used to estimate

the likelihood that any particular frame is likely to be sufficiently accurate with frames wherein too few markers or too large a marker error are detected being discarded. This requires the capture and processing rate to be in advance of the display rate to the user (expected to be >10fps for smooth viewing and low latency) which in turn affects the amount of computational power required by the DGS unit.

It is believed that there is also potential for increasing the system accuracy through better controlling the lighting, modifications to the corner refinement technique to use all edge pixels rather than simply the identified corner or optimising the camera lens combination. It would also be possible to provide a large accuracy gain through replacing the single camera in the current system with a stereo camera setup as originally discussed in [8], this would have drawbacks for the cost, size and computational power of the DGS but does provide a means of increasing accuracy if required and would provide a solution to the mirroring of the Z-axis.

6 Conclusion

The use of fiducial markers to aid in the accurate and fast placement of screws or K-wires in orthopaedic surgery appears to be achievable using single camera systems with an accuracy of 0.45±0.56mm being measured in laboratory testing when there is 300mm between markers and camera. If proven this method could also reduce the radiation exposure of those in surgery by reducing or eliminating the use of fluoroscopy. To achieve these results individual fiducial markers were replaced with boards composed of 4 markers and the parameters of the sub-pixel refinement method were optimised. As the distance between the marker and camera increases there was a corresponding reduction in accuracy which would provide a limit on the systems useable range. The biggest limitation of the single camera approach is the ability for any object to have two possible pose's with mirrored z-axis. This challenge should be minimised in real-time operation where the flipping between the two pose's should be easily detectable frame-to-frame due to the unrealistic motion implied. A number of ideas for further improvement to the accuracy of the DGS are currently being investigated including improved lighting, varying camera and lens combinations and modifications to the corner location algorithm.

There also remain a number of other challenges to the realisation of a field-testable solution, including achieving sufficiently high frame rates whilst minimising the device size, making the device suitable for sterilisation and providing error checking to detect those frames that provide extremely inaccurate results (>10mm). Work is on-going with a view to conducting initial clinical trials in 2020.

6.1 Compliance with ethical standards

Conflict of interest: The authors declare that they have no conflict of interest.

Ethical Approval: This article does not contain any studies with human participants or animals performed by any of the authors."

Informed Consent: This articles does not contain patient data.

Funding: This research was funded the National Institute for Health Research (NIHR)'s Invention for Innovation (i4i) Programme under grant II-LA-1116-20004.

Acknowledgements This is a summary of independent research funded by the National Institute for Health Research (NIHR)'s Invention for Innovation (i4i) Programme under grant II-LA-1116-20004. The views expressed are those of the author(s) and not necessarily those of the NHS, the NIHR or the Department of Health.

References

1. Alici, G., Daniel, R.W.: Robotic drilling under force control: execution of a task. In: Intelligent Robots and Systems' 94.'Advanced Robotic Systems and the Real World', IROS'94. Proceedings of the IEEE/RSJ/GI International Conference on. vol. 3, pp. 1618–1625. IEEE (1994)
2. Allotta, B., Giacalone, G., Rinaldi, L.: A hand-held drilling tool for orthopedic surgery. IEEE/ASME Transactions on Mechatronics **2**(4), 218–229 (1997)
3. Arora, R., Lutz, M., Hennerbichler, A., Krappinger, D., Espen, D., Gabl, M.: Complications following internal fixation of unstable distal radius fracture with a palmar locking-plate. Journal of Orthopaedic Trauma **21**(5), 316–322 (may 2007). https://doi.org/10.1097/BOT.0b013e318059b993, `https://insights.ovid.com/crossref?an=00005131-200705000-00005`
4. Belongie, S.: Rodrigues rotation formula. From MathWorld– created by Eric W. Weisstein. http://mathworld.wolfram.com/RodriguesRotationFormula.html (1999)
5. Bertelsen, A., Melo, J., Sánchez, E., Borro, D.: A review of surgical robots for spinal interventions. The International Journal of Medical Robotics and Computer Assisted Surgery **9**(4), 407–422 (2013)
6. Bond, C.D., Shin, A.Y., McBride, M.T., Dao, K.D.: Percutaneous screw fixation or cast immobilization for nondisplaced scaphoid fractures. JBJS **83**(4), 483 (2001)
7. Esses, S.I., Sachs, B.L., Dreyzin, V.: Complications associated with the technique of pedicle screw fixation. a selected survey of abs members. Spine **18**(15), 2231–8 (1993)
8. Georgilas, I., Giddins, G., Du Bois, J.: Towards accurate drilling guidance for orthopaedic surgery. In: Joint Workshop on New Technologies for Computer/Robot Assisted Surgery (CRAS) (2018)
9. Lonner, J.H.: Robotically assisted unicompartmental knee arthroplasty with a handheld image-free sculpting tool. Operative techniques in orthopaedics **25**(2), 104–113 (2015)
10. Louredo, M., Díaz, I., Gil, J.J.: Dribon: A mechatronic bone drilling tool. Mechatronics **22**(8), 1060–1066 (2012)
11. Lowe, J.B., Monazzam, S., Walton, B., Nelson, E., Wolinsky, P.R.: How to use fluoroscopic imaging to prevent intraarticular screw perforation during locked plating of proximal humerus fractures: A cadaveric study. Journal of Orthopaedic Trauma **29**(10), e401–e407 (oct 2015). https://doi.org/10.1097/BOT.0000000000000333, `http://content.wkhealth.com/linkback/openurl?sid=WKPTLP:landingpage{&}an=00005131-201510000-00023`
12. Pearle, A.D., Kendoff, D., Stueber, V., Musahl, V., Repicci, J.A.: Perioperative management of unicompartmental knee arthroplasty using the mako robotic arm system (makoplasty). American Journal of Orthopedics **38**(2), 16–19 (2009)

13. Romero-Ramirez, F.J., Muoz-Salinas, R., Medina-Carnicer, R.: Speeded up detection of squared fiducial markers. Image and Vision Computing **76**, 38 – 47 (2018)
14. Salinas, R.M.: Aruco. Universidad de Crdoba (2018), https://tinyurl/ArucoDoc
15. Shim, S., Choi, H., Ji, D., Kang, W., Hong, J.: Robotic system for bone drilling using a rolling friction mechanism. IEEE/ASME Transactions on Mechatronics **23**(5), 2295–2305 (2018)